Peer-reviewed version available at *Materials* **2020**, *13*, 876; doi:10.3390/ma13040876

Use of a Hydroalcoholic Extract of *Moringa oleifera* Leaves for the Green Synthesis of Bismuth Nanoparticles and Evaluation of Their Anti-Microbial and Antioxidant Activities

Prince Edwin Das,[1] Amin F. Majdalawieh,[2]* Imad A. Abu-Yousef,[2] Srinivasan Narasimhan,[1]* and Palmiro Poltronieri[3]*

[1]Asthagiri Herbal Research Foundation, 162A, Perungudi Industrial Estate, Perungudi, Chennai, India 600096. E-mails: prince.ahrf@gmail.com (P.E.D.); asthagiri.herbal@gmail.com (S.N.)

[2]Department of Biology, Chemistry and Environmental Sciences, American University of Sharjah, P.O. Box 26666, Sharjah, United Arab Emirates, E-mails: amajdalawieh@aus.edu (A.F.M); iabuyousef@aus.edu (I.A.A.Y)

[3]Institute of Sciences of Food Productions, CNR-ISPA, Lecce 73100, Italy. E-mail: palmiro.poltronieri@ispa.cnr.it (P.P.)

**Corresponding Author.* A.F. Majdalawieh: Phone: (971) 6 5152429; Fax: (971) 6 515 2450. E-mail: amajdalawieh@aus.edu; S. Narasimhan: Phone: (91) 44 22397645; Fax: (91) 44 22397645. E-mail: narasimhan_s@yahoo.com; asthagiri.herbal@gmail.com

Peer-reviewed version available at *Materials* **2020**, *13*, 876; doi:10.3390/ma13040876

Abstract

The use of plant extracts in the synthesis of metal nanoparticles is a very attractive approach in the field of green synthesis. To benefit from the potential synergy between the biological activities of the *Moringa oleifera* (MO) leaves extract and metallic bismuth, our study aimed at synthesizing bismuth nanoparticles using a hydroalcoholic extract of *M. oleifera* leaves as a means of green synthesis that yields nontoxic products and reduces the production of wasteful material. To this end, the *M. oleifera* leaves extract was treated with a bismuth nitrate pentahydrate solution. A color change from light brown to dark brown indicates the synthesis of bismuth nanoparticles. The total phenolic content in the *M. oleifera* leaves extract used was 23.0 ± 0.3 mg gallic acid equivalent/g of dried *M. oleifera* leaves powder. Antioxidant property of MO synthesised bismuth Nanoparticles was evaluated and in line with the extract used in the synthesis of NPs.

The physical properties of the synthesized bismuth nanoparticles were characterized using UV-Vis spectrophotometer, FT-IR spectrometer, TEM, SEM, and XRD. The synthesized bismuth nanoparticles have a size in the range of 40.4-57.8 nm with amorphous morphology. Using DPPH and phosphomolybdate assays, our findings revealed that the *M. oleifera* leaves extract and the synthesized bismuth nanoparticles possess antioxidant properties.

Using resazurin microtiter assay, we also demonstrate that the *M. oleifera* leaves extract and the synthesized bismuth nanoparticles exert potent anti-bacterial activity against *Escherichia coli, Klebsiella pneumoniae, Staphylococcus aureus* and *Enterococcus faecalis*, similarly to the inhibition exerted by Moringa extract, especially against *E. faecalis* (MIC values for the extract: 500, 250, 250, and 250 µg/mL; MIC values for the bismuth nanoparticles: 500, 500, 500, and 250 µg/mL, respectively). Similarly, the *M. oleifera* leaves extract and the synthesized bismuth nanoparticles display relatively stronger anti-fungal activity against *Aspergillus niger, Aspergillus flavus, Candida albicans* and *Candida glabrata* (MIC values

Peer-reviewed version available at *Materials* **2020**, *13*, 876; doi:10.3390/ma13040876

for the extract: 62.5, 62.5, 125, and 250 µg/mL; MIC values for the bismuth nanoparticles: 250, 250, 62.5, and 62.5 µg/mL, respectively). Thus, the hydroalcoholic extract of *M. oleifera* leaves was successfully used in the synthesis of bismuth nanoparticles, showing a positive antioxidant, anti-bacterial, and anti-fungal activity. Therefore, the synthesized bismuth nanoparticles can potentially be employed in the alleviation of symptoms associated with oxidative stress and in the topic treatment of Candida infections.

Keywords: *Moringa oleifera*; bismuth nanoparticles; polyphenolics; anti-bacterial; anti-fungal; antioxidant

1. Introduction

Moringa oleifera (family Moringaceae) is one of the most studied herbs. It is considered to be a sacred plant and referred to as the "tree of life" in several cultures. It has been widely cultivated in various parts of the world and for many decades because of its potential use in numerous applications in industry, pharmacy, and medicine. Both its leaves and fruits are used in cooking, and they are part of many cuisines worldwide. Moreover, many home remedies and traditional medicinal formulations are prepared using all parts of *M. oleifera* [1]. Its leaves are edible and they are of considerable nutritional and therapeutic value due to their rich vitamin and amino acid content [2]. Experimental evidence suggests that the diverse medical applications of *M. oleifera* leaves can be partially attributed to the antioxidant potential of the phenolic compounds present in the leaves [3]. For many years, plant-based compounds and their derivatives have been used in the manufacturing of textiles, fabrics, polymers for food and non-food applications, biomaterials for oral hygiene and prevention of dental caries and biofilm formation, and foil polymers for food wrapping and packaging [4-9]. The antimicrobial and antioxidant properties of silver and other metallic nanoparticles forced

Peer-reviewed version available at *Materials* **2020**, *13*, 876; doi:10.3390/ma13040876

the development of several new nanomaterials followed by the evaluation of their biological activities [10-15].

Several active compounds (e.g. proteins, flavonoids and carboxylic groups of arabinose and galactose, reducing sugars, tannins, aliphatic amines, aliphatic alkenes of alkaloids, polysaccharides, aromatic amines, sec-alcohols, water-soluble heterocyclic components and saponins) isolated from plant extracts have been employed in the successful synthesis of silver nanoparticles [16]. Individually, many plant extracts and metallic nanoparticles are known to possess significant biological activities both *in vitro* and *in vivo*. As such, it is envisioned that the green synthesis of metallic nanoparticles using plant extracts may cause a synergistic effect leading to more robust biological activities. Hence, the use of plant extracts to synthesize metallic nanoparticles may lead to the formation of new nanomaterial with more potent and/or novel biological activities [17]. Indeed, several studies demonstrate the successful synthesis of gold and silver nanoparticles using the leaves' extracts of *Erythrina suberosa (Roxb.)*, *Paederia foetida*, *Acalypha indica*, *Cassia auriculata*, *Sorbus aucuparia*, and *Azadirachta indica*, and their antimicrobial activities were assessed and confirmed [18-23]. Along the same line, other studies demonstrated that silver nanoparticles that were synthesized using various plant extracts exert potent antioxidant activity [24-28].

Bismuth nanoparticles, with a size of 25 nm, were successfully synthesized by the laser ablation method, and they can be employed as high contrast medium for high-resolution imaging in biological systems [29]. Notably, bismuth nanoparticles ~~that are~~ synthesized by conventional solvent techniques have a size in the range of 50-103 nm with a very high anti-wear property [30]. Bismuth nanoparticles are also used as catalysts in reduction of nitro compounds to azo compounds [31]. Bismuth nanoparticles, with a size of 40 nm, ~~that~~ were synthesised by colloidal-chemical method in water medium, were shown to exert potent anti-microbial activity against several pathogenic microorganisms [32].

Bismuth nanoparticles with better catalytic activity were synthesized by the redox reactions between sodium borohydride and ammonium bismuth citrate in the presence of soluble starch in aqueous phase [33]. Bismuth nanodots were synthesized by the redox reaction between bismuth nitrate and D-glucose, in the presence of polyvinylpyrrolidone in the basic aqueous phase. The reduction of 4-nitrophenol to 4-aminophenol requires only 36 µg/mL nano-catalyst for 20 mM of the substrate [34]. The nanostructured Ag-Bi alloys were prepared by a mechano-chemistry pathway under normal conditions and with minimum amount of solvent. These nanostructured Ag-Bi alloys effectively degraded NO but they were rapidly oxidized [35].Bismuth nanoparticles-decorated multi-wall carbon nano-tubes were synthesized and modified carbon paste electrodes were fabricated to serve as a novel amperometric sensor for the detection of gallic acid. This sensor estimates gallic acid in cloves and green tea extracts with complete elimination of interferences [36]. Zerovalent bismuth nanoparticles were synthesized by a two-pot synthesis based on a combination of cementation process and a wet ball-stirring process [37]. High-contrast medium for high-resolution imaging in biological systems was developed using the bismuth nanoparticles synthesized by laser ablation in aqueous medium [38]. Numerous studies were reported on the synthesis and characterization of bismuth oxide, bismuth sulfide, and spherical bismuth metallic nanoparticles. The various strategies and different capping agents were used to control the size, morphology, and stability of these nanoparticles. In the medical field, bismuth nanoparticles were used as an X-ray contrast agent [39]. Under a low X-ray dose, a radiosensitizer composed of bismuth nanoparticles conjugated to antibodies was used to specifically target and kill multidrug resistant bacteria [39].

Herein, we attempted to achieve enhanced biological activities of bismuth nanoparticles via their synthesis using *M. oleifera* leaves' phytochemical constituents. To this end, we pursued green synthesis of bismuth nanoparticles using a hydroalcoholic extract of *M. oleifera* leaves,

Peer-reviewed version available at *Materials* **2020**, *13*, 876; doi:10.3390/ma13040876

followed by their physical characterization using different techniques. We also assessed the antioxidant activity of the *M. oleifera* leaves extract and the synthesized bismuth nanoparticles as well as their anti-bacterial and anti-fungal activities against different species of bacteria and fungi. We anticipate that our findings will be significant in the employment of green-synthesized bismuth nanoparticles in several medical applications.

2. Results and Discussion

2.1. Phytochemical Analysis of the *M. oleifera* Leaves Extract

The qualitative evaluation of different chemical constituents in the *M. oleifera* leaves extract was performed using the test methods indicated in Table 1. The protein content in the *M. oleifera* leaves extract was estimated to be 0.1% of the dry leaves powder. The total phenolic content in *M. oleifera* leaves extract was 23% of the dry leaves powder. An earlier study demonstrated that alanine, tyrosine, lysine, and threonine are among the major amino acids present in the *M. oleifera* leaves extract [40]. The concoction of *M. oleifera* leaves extract contains isomers of ceffeoylquinic acid, isomers of feruloylquinic acid, tannins, gallic acid, and several flavonoids like quercetin, kaempferol and their glycoside derivatives [41]. Using HPLC analysis, crypto-chlorogenic acid, isoquercetin, and astragalin were identified in the ethanolic extract of *Moringa oleifera* leaves [42]. The hydroalcoholic extract of *Moringa oleifera* leaves, having water and ethanol (50:50), contains numerous unexplored macromolecules. Collectively, these findings suggest that the *M. oleifera* leaves extract could serve as a nutritional supplement and a possible stabilizing agent for the formed bismuth nanoparticles.

Preprints (www.preprints.org) | NOT PEER-REVIEWED | Posted: 21 December 2019 doi:10.20944/preprints201912.0286.v1

Peer-reviewed version available at *Materials* **2020**, *13*, 876; doi:10.3390/ma13040876

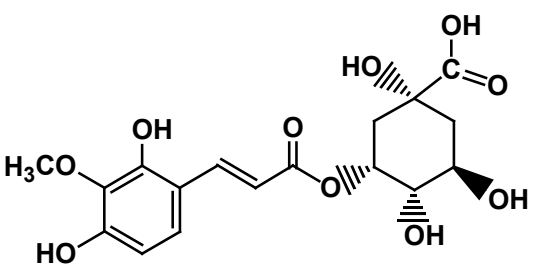

Feruloylquinic acid

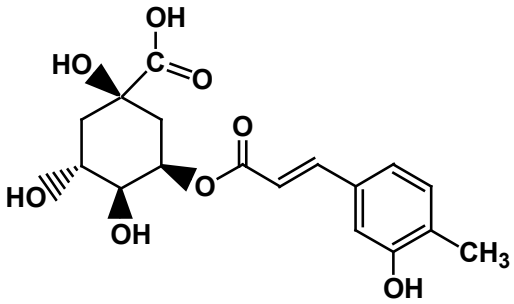

Ceffeoylquinic acid

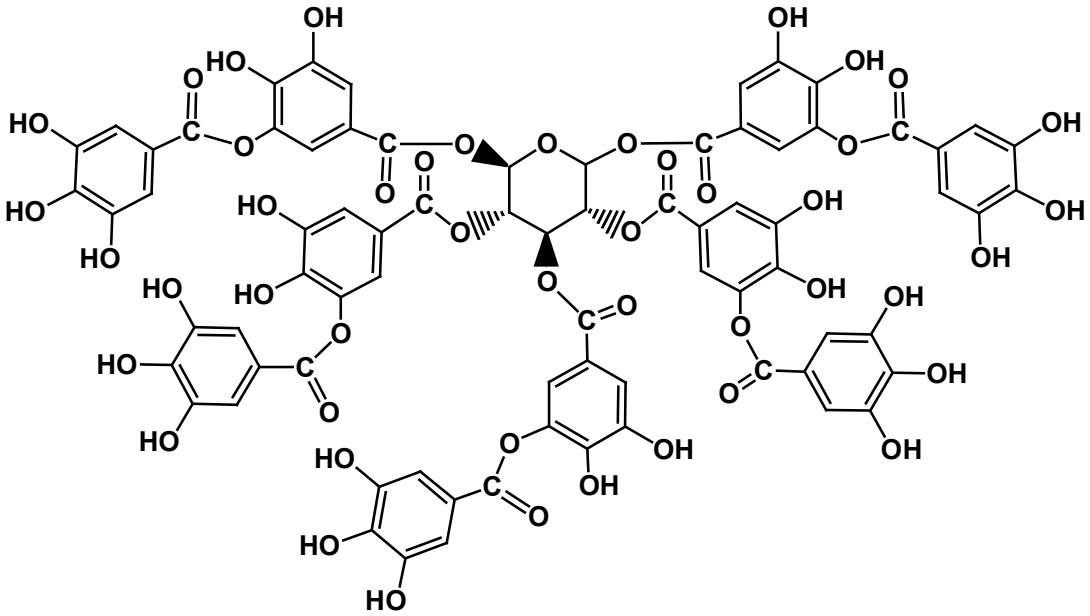

Tannins

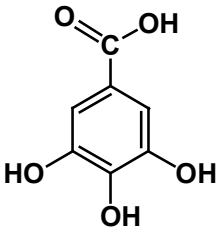

Gallic acid

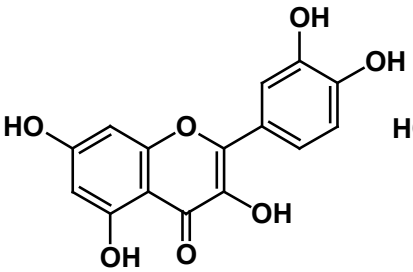

Quercetin

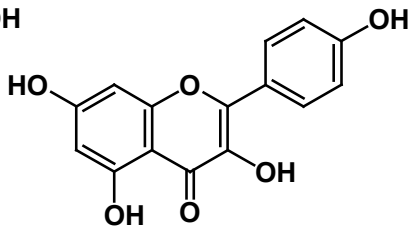

Kaempferol

Table 1. Phytochemical analysis of the *M. oleifera* leaves extract. The presence of the indicated chemical constituents is indicated with (+).

Chemical constituents	Test method	*M. oleifera* leaves extract

Preprints (www.preprints.org) | NOT PEER-REVIEWED | Posted: 21 December 2019 doi:10.20944/preprints201912.0286.v1

Peer-reviewed version available at Materials 2020, 13, 876; doi:10.3390/ma13040876

Alkaloids	Dragendroff's test	+
Tannins	Ferric chloride	+
Flavonoids	Shinoda test	+
Steroids	Salkowski reaction	+
Saponins	Foam test	+
Polyphenols	Puncal-D	+
Glycosides	Conc. H_2SO_4 and heat	+
Carbohydrates	Anthrone test	+
Proteins	Ninhydrin test	+
Amino acids	Millon's test	+

From the total phenolic content estimation of the *M. oleifera* leaves extract before and after the reaction (Table 2), Scheme 1 is proposed. The total phenolic content of 60 mg gallic acid equivalent from 10 g of dried *M. oleifera* leaves powder was used in the synthesis of 170 mg of bismuth nanoparticles from 0.04 M of bismuth (III) ion solution. The other reducing and binding chemical entities present in the concoction aid in the formation and stabilization of the synthesized bismuth nanoparticles.

Table 2. Estimation of total phenolic content before and after the synthesis of bismuth nanoparticles.

Sample	**Total phenolic content (mg/g of dried leaves)**
M. oleifera leaves extract (before synthesis)	23.0 ± 0.3

M. oleifera leaves extract (after synthesis)	17.0 ± 0.4

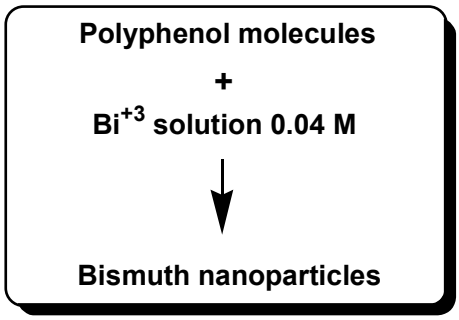

Scheme 1. Schematic representation of the synthesis of bismuth nanoparticles.

2.2. Characterization

2.2.1. Size and Morphology of the Synthesized Bismuth Nanoparticles

The synthesized bismuth nanoparticles were imaged using JEOL-TEM (JEM) (Figure 1) and energy dispersive X-ray spectroscopy (EDS) (Figure 2).

Preprints (www.preprints.org) | NOT PEER-REVIEWED | Posted: 21 December 2019 doi:10.20944/preprints201912.0286.v1

Peer-reviewed version available at Materials 2020, 13, 876; doi:10.3390/ma13040876

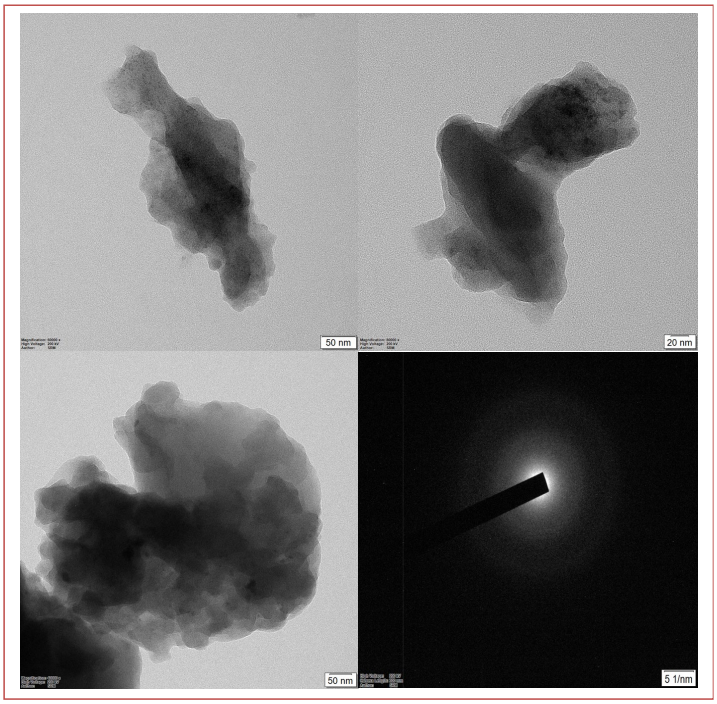

Figure 1. JEOL-TEM (JEM) images of the synthesized bismuth nanoparticles.

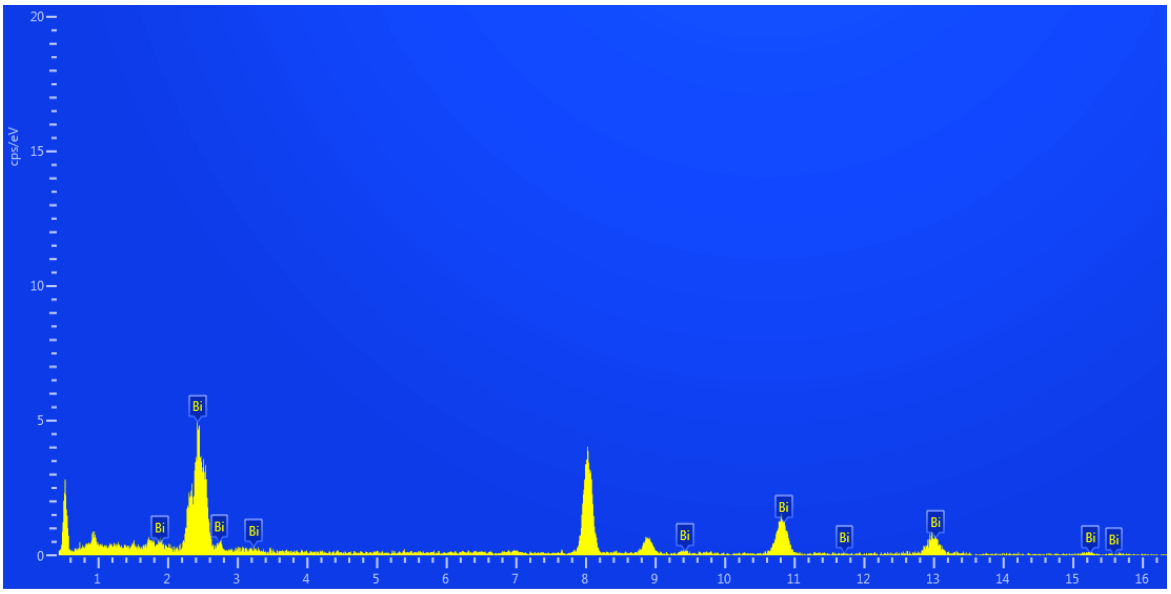

Figure 2.EDS spectrum with peaks corresponding to bismuth.

The synthesized bismuth nanoparticles were obtained in ethanol to give a colloidal solution. The synthesized bismuth nanoparticles are amorphous in nature and they agglomerate upon

Peer-reviewed version available at *Materials* **2020**, *13*, 876; doi:10.3390/ma13040876

storage. The energy dispersive X-ray spectroscopy analysis (EDS) confirmed the presence of the elemental bismuth nanoparticles. The absence of other elemental peaks reflects the purity of the sample. The SEM images (Figure 3) indicate that the size of the synthesized bismuth particles is 40.4-57.8 nm.

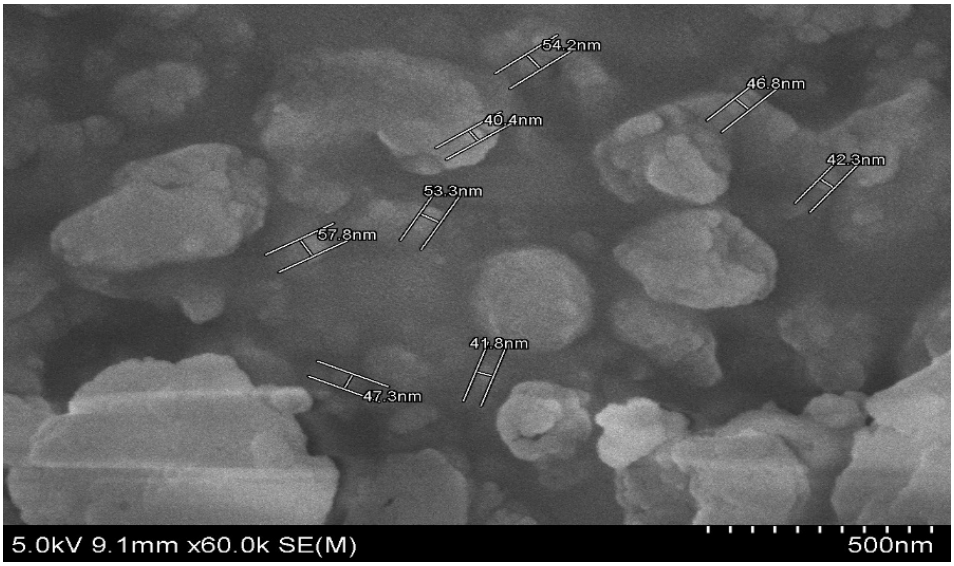

Figure 3. SEM image of the synthesized bismuth nanoparticles.

X-ray diffraction (XRD) analysis confirms the amorphous nature of the synthesized bismuth nanoparticles (Figure 4). This substantiates the diffraction pattern observed in the JEOL-TEM (JEM) images (Figure 1), suggesting that the synthesized bismuth nanoparticles are amorphous in morphology.

Preprints (www.preprints.org) | NOT PEER-REVIEWED | Posted: 21 December 2019 doi:10.20944/preprints201912.0286.v1

Peer-reviewed version available at Materials 2020, 13, 876; doi:10.3390/ma13040876

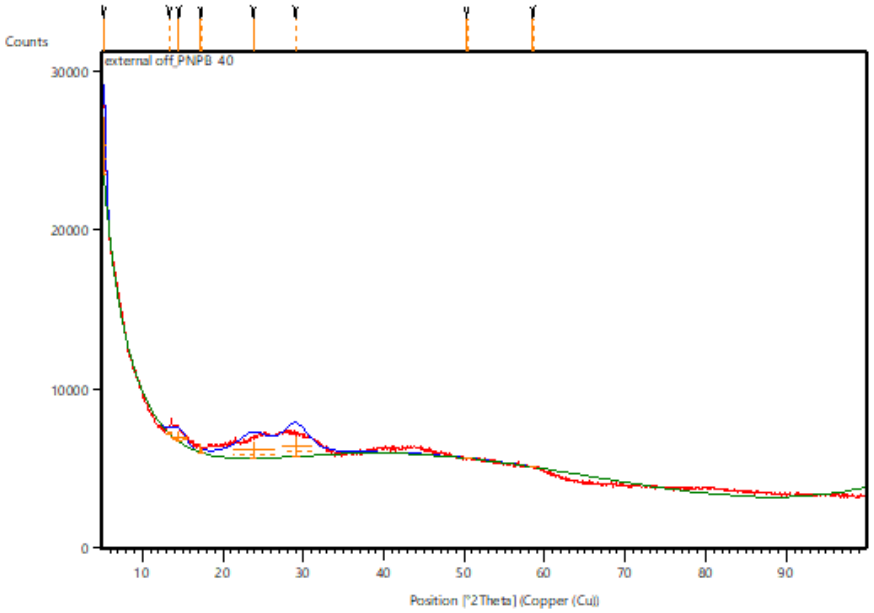

Figure 4. XRD spectrum of the synthesized bismuth nanoparticles.

2.2.2. Fourier Transform Infrared Spectroscopy (FT-IR) of the *M. oleifera* Leaves Extract and the Synthesized Bismuth Nanoparticles

The FT-IR spectra of the *M. oleifera* leaves extract and the synthesized bismuth nanoparticles are shown in Figure 5 and Figure 6, respectively. This vibration spectroscopy data can be used to understand the biomolecules involved in the synthesis of bismuth nanoparticles. The bands around 3400 cm^{-1} and 1630 cm^{-1} are broad in the *M. oleifera* leaves extract (Figure 5), corresponding to the vibration mode of hydroxyl group, mostly found in polyphenolic molecules such as tannins, flavonoids, and glycoside derivatives. The FT-IR spectrum of the synthesized bismuth nanoparticles (Figure 6) depicts a sharp band at 3431 cm^{-1}, corresponding to the N-H vibration mode. The fingerprint region at 1269 cm^{-1} explains the binding of the organic matrix to the synthesized bismuth nanoparticles. This comparison reflects the participation of the hydroxyl group in the synthesis of bismuth nanoparticles. Moreover, the binding characteristics of amino groups in the *M. oleifera* leaves extract are

Preprints (www.preprints.org) | NOT PEER-REVIEWED | Posted: 21 December 2019 doi:10.20944/preprints201912.0286.v1

Peer-reviewed version available at Materials 2020, 13, 876; doi:10.3390/ma13040876

observed in Figure 5 and Figure 6. This could be the reason for agglomeration of the synthesized bismuth nanoparticles to give an amorphous morphology.

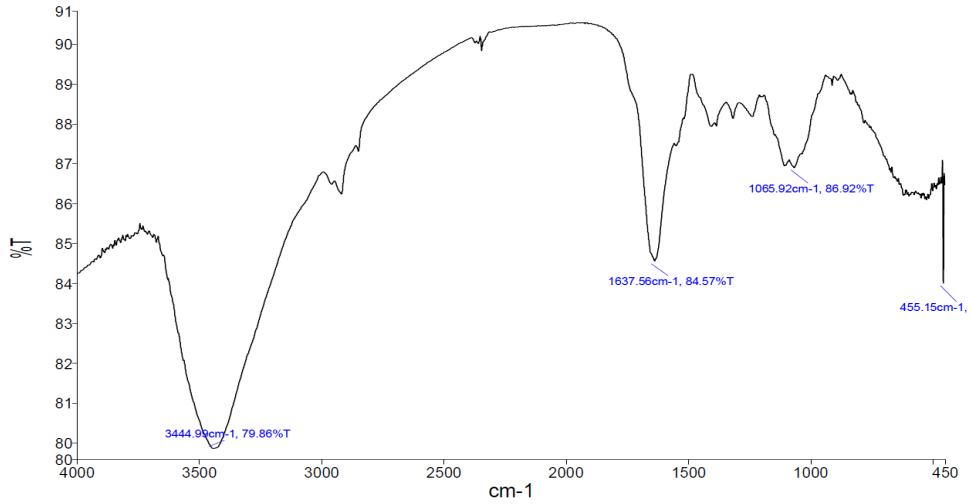

Figure 5. FT-IR spectrum of the *M. oleifera* leaves extract.

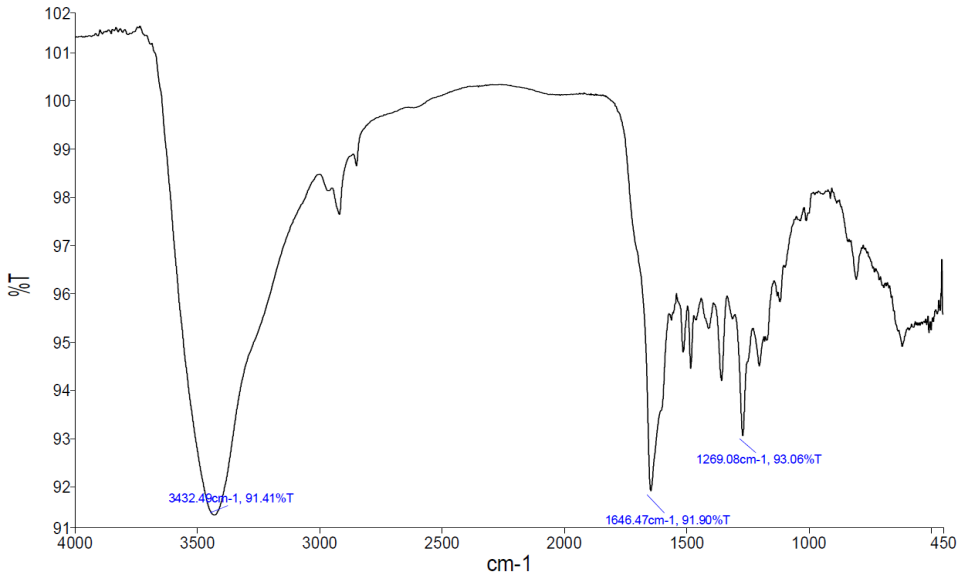

Figure 6. FT-IR spectrum of the synthesized bismuth nanoparticles.

2.2.3. UV-Vis Spectroscopy of the *M. oleifera* Leaves Extract and the Synthesized Bismuth Nanoparticles

Preprints (www.preprints.org) | NOT PEER-REVIEWED | Posted: 21 December 2019 doi:10.20944/preprints201912.0286.v1

Peer-reviewed version available at Materials 2020, 13, 876; doi:10.3390/ma13040876

The UV-Vis absorption spectrum of the *M. oleifera* leaves extract is shown in Figure 7, λ_{max} at 390 nm. The UV-Vis spectrum of the synthesized bismuth nanoparticles reconstituted in dimethyl sulfoxide (DMSO) solvent is shown in Figure 8, λ_{max} at 270 nm.

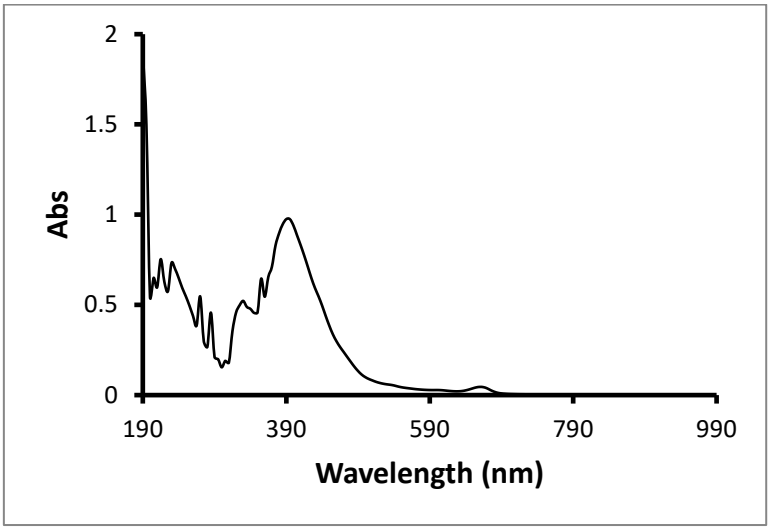

Figure 7. UV-Vis spectrum of the *M. oleifera* leaves extract.

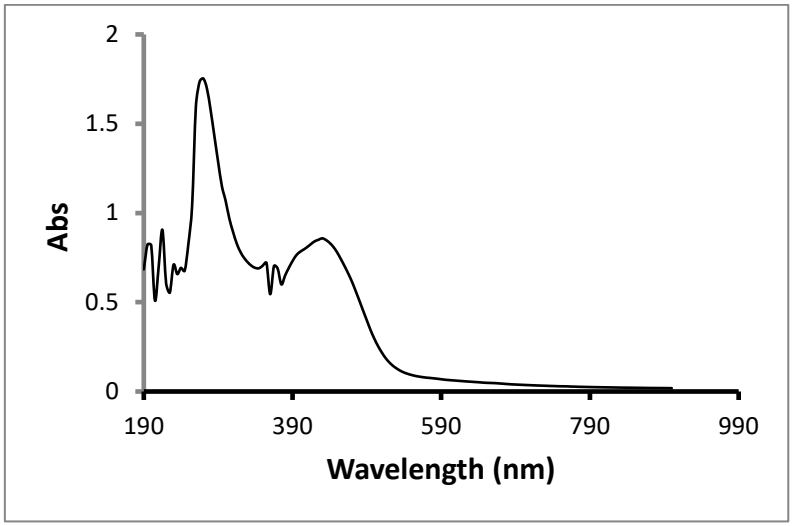

Figure 8. UV-Vis spectrum of the synthesized bismuth nanoparticles.

2.3. Antioxidant Activity of the *M. oleifera* Leaves Extract and the Synthesized Bismuth Nanoparticles

Preprints (www.preprints.org) | NOT PEER-REVIEWED | Posted: 21 December 2019 doi:10.20944/preprints201912.0286.v1

Peer-reviewed version available at Materials 2020, 13, 876; doi:10.3390/ma13040876

Using DPPH assay against ascorbic acid as a standard, the percentage of antioxidant activity of the *M. oleifera* leaves extract and the synthesized bismuth nanoparticles was assessed. As shown in Table 3, the *M. oleifera* leaves extract exerted considerable antioxidant activity, while the synthesized bismuth nanoparticles displayed relatively weaker antioxidant activity. These results were supported with total antioxidant capacity measured by phosphomolybdate assay (Table 4).

Table 3. Antioxidant activity percentage (AA%) using DPPH assay.

Sample	**Amount (µg)**				
	100	**200**	**300**	**400**	**500**
Ascorbic acid (standard)	34.4	55.1	67.2	75.8	84.4
M. oleifera leaves extract	55.1	58.6	63.7	65.5	65.5
Bismuth nanoparticles	25.8	37.9	37.9	48.2	60.3

Table 4. Total antioxidant capacity (TAC) using phosphomolybdate assay.

Sample	**Concentration (µg/mL) (Ascorbic acid equivalent)**				
	200	**400**	**600**	**800**	**1000**
M. oleifera leaves extract	130	260	410	530	690
Bismuth nanoparticles	50	50	50	60	60

2.4. Anti-Bacterial Activity of the *M. oleifera* Leaves Extract and the Synthesized Bismuth Nanoparticles

The potential anti-bacterial activity of synthesized bismuth nanoparticles was evaluated against *E. coli*, *K. pneumoniae*, *S. aureus*, and *E. faecalis*. Streptomycin (10 µg/500 µL) was

Peer-reviewed version available at *Materials* **2020**, *13*, 876; doi:10.3390/ma13040876

used as a positive control, while water-ethanol (1:1) solution and DMSO solvent were used as negative controls for the *M. oleifera* leaves extract and the bismuth nanoparticles, respectively. The nutrient broth was also used as a negative control. The classification of these species of bacteria and their localization in the human body is given in Table 5. The minimum inhibitory concentration (MIC) values measured in presence of the *M. oleifera* leaves extract and the bismuth nanoparticles are given in Table 6. The growth of the indicated species of bacteria in presence of different concentrations (7.8-1000 µg/mL) of *M. oleifera* leaves extract and the bismuth nanoparticles is shown in Table 7. The resazurin microtiter assay plates for the *M. oleifera* leaves extract and the bismuth nanoparticles are shown in Figure 9. In presence of the *M. oleifera* leaves extract, the MIC values against *E. coli*, *K. pneumoniae*, *S. aureus*, and *E. faecalis* were found to be in the range of 250-500 µg/mL (Table 6). Very similar MIC values (250-500 µg/mL) were observed in presence of the synthesized bismuth nanoparticles (Table 6), indicating that *M. oleifera* leaves extract and the bismuth nanoparticles have comparable anti-bacterial activities (Table 7 and Figure 9).

Table 5. Species of bacteria used for the anti-bacterial study.

No.	Bacterial species	Classification	Localization in the human body
1	*Escherichia coli*	Gram-negative	Lower intestine
2	*Klebsiella pneumoniae*	Gram-negative	Flora in the mouth, skin, and intestines
3	*Staphylococcus aureus*	Gram-positive	Upper respiratory track and skin
4	*Enterococcus faecalis*	Gram-positive	Gastrointestinal tract

Preprints (www.preprints.org) | NOT PEER-REVIEWED | Posted: 21 December 2019 doi:10.20944/preprints201912.0286.v1

Peer-reviewed version available at Materials 2020, 13, 876; doi:10.3390/ma13040876

Table 6. Anti-bacterial activity (MIC values).

Bacterial species	MIC (µg/mL)
***M. oleifera* leaves extract**	
Escherichia coli	500
Klebsiella pneumoniae	250
Staphylococcus aureus	250
Enterococcus faecalis	250
Bismuth nanoparticles	
Escherichia coli	500
Klebsiella pneumoniae	500
Staphylococcus aureus	500
Enterococcus faecalis	250

Table 7. Anti-bacterial activity data (growth (+) and no growth (-)).

No.	Bacterial species	Growth of bacteria										
	Concentration (µg/mL)	1000 (1)	500 (2)	250 (3)	125 (4)	62.5 (5)	31.2 (6)	15.6 (7)	7.8 (8)	Streptomycin	Negative	Nutrient broth
	***M. oleifera* leaves extract**											
1	*Escherichia coli*	-	-	+	+	+	+	+	+	-	+	+
2	*Klebsiella pneumoniae*	-	-	-	+	+	+	+	+	-	+	+

Preprints (www.preprints.org) | NOT PEER-REVIEWED | Posted: 21 December 2019 doi:10.20944/preprints201912.0286.v1

Peer-reviewed version available at *Materials* **2020**, *13*, 876; doi:10.3390/ma13040876

3	*Staphylococcus aureus*	-	-	-	+	+	+	+	+	-	+	+
4	*Enterococcus faecalis*	-	-	-	+	+	+	+	+	-	+	+
	Bismuth Nanoparticles											
1	*Escherichia coli*	-	-	+	+	+	+	+	+	-	+	+
2	*Klebsiella pneumoniae*	-	-	+	+	+	+	+	+	-	+	+
3	*Staphylococcus aureus*	-	-	+	+	+	+	+	+	-	+	+
4	*Enterococcus faecalis*	-	-	-	+	+	+	+	+	-	+	+

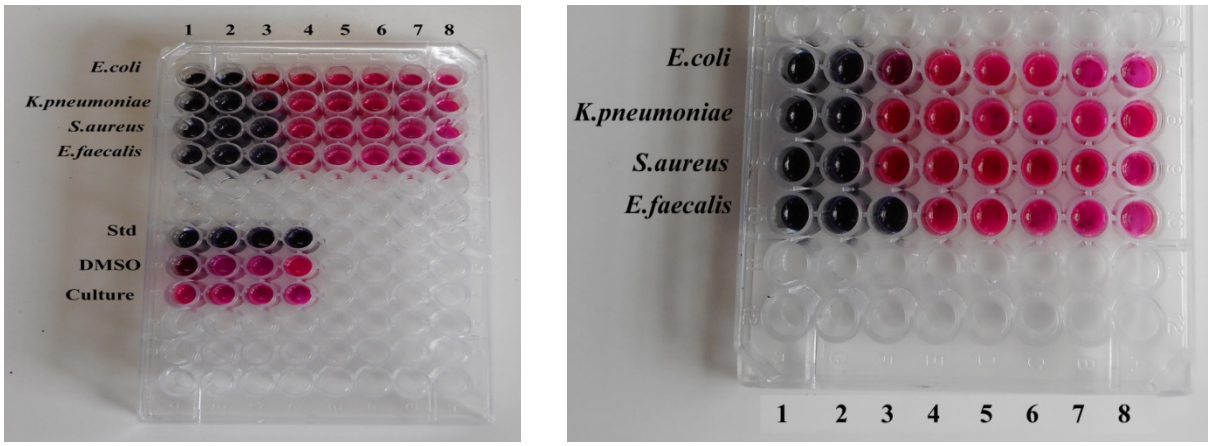

M. oleifera leaves extract Bismuth Nanoparticles

Figure 9. Resazurin microtiter assay plates for the *M. oleifera* leaves extract and the synthesized bismuth nanoparticles.

Peer-reviewed version available at *Materials* **2020**, *13*, 876; doi:10.3390/ma13040876

2.5. Anti-Fungal Activity of the *M. oleifera* Leaves Extract and the Synthesized Bismuth Nanoparticles

The potential anti-fungal activity of synthesized bismuth nanoparticles was evaluated against *A. niger*, *A. flavus*, *C. albicans* and *C. glabrata*. Ketoconazole (10 µg/500 µL) was used as a positive control, while water-ethanol (1:1) solution and DMSO solvent were used as negative controls for the *M. oleifera* leaves extract and the bismuth nanoparticles, respectively. The nutrient broth was also used as a negative control. The classification of these species of fungi and their localization in the human body is given in Table 8. The minimum inhibitory concentration (MIC) values measured in presence of the *M. oleifera* leaves extract and the bismuth nanoparticles are given in Table 9. The growth of the indicated species of fungi in presence of difference concentrations (7.8-1000 µg/mL) of *M. oleifera* leaves extract and the bismuth nanoparticles is shown in Table 10. The resazurin microtiter assay plates for the *M. oleifera* leaves extract and the bismuth nanoparticles are shown in Figure 10. In presence of the *M. oleifera* leaves extract, the MIC values against *A. niger*, *A. flavus*, *C. albicans* and *C. glabrata* were found to be 62.5, 62.5, 125, and 250 µg/mL, respectively (Table 9). In presence of the synthesized bismuth nanoparticles, the MIC values against *A. niger*, *A. flavus*, *C. albicans* and *C. glabrata* were found to be 250, 250, 62.5, and 62.5 µg/mL, respectively (Table 9). These findings indicate that the bismuth nanoparticles displayed more effective anti-fungal activity against *C. albicans* and *C. glabrata* compared to the *M. oleifera* leaves extract (Table 9, Table 10, and Figure 10). Candida species are normally present on human skin, and their infections are common in skin and other tissues due to ineffective immune responses. The synthesized bismuth nanoparticles could be a promising therapeutic candidate to treat candidiasis after considering their pharmacokinetics.

Preprints (www.preprints.org) | NOT PEER-REVIEWED | Posted: 21 December 2019 doi:10.20944/preprints201912.0286.v1

Peer-reviewed version available at Materials 2020, 13, 876; doi:10.3390/ma13040876

Table 8. Species of fungi used for the anti-fungal study.

No.	Fungal species	Localization in the human body
1	*Aspergillus niger*	Lungs
2	*Aspergillus flavus*	Lungs, eyes, and ears
3	*Candida albicans*	Flora in gastrointestinal tract
4	*Candida glabrata*	Mucosal tissues

Table 9. Anti-fungal activity (MIC values).

Fungal species	MIC (µg/mL)
***M. oleifera* leaves extract**	
Aspergillus niger	62.5
Aspergillus flavus	62.5
Candida albicans	125
Candida glabrata	250
Bismuth nanoparticles	
Aspergillus niger	250
Aspergillus flavus	250
Candida albicans	62.5
Candida glabrata	62.5

Table 10. Anti-fungal activity data (growth (+) and no growth (-)).

No.	Fungal species	Growth of fungi

Preprints (www.preprints.org) | NOT PEER-REVIEWED | Posted: 21 December 2019 doi:10.20944/preprints201912.0286.v1

Peer-reviewed version available at Materials 2020, 13, 876; doi:10.3390/ma13040876

	Concentration (µg/mL)	1000 (1)	500 (2)	250 (3)	125 (4)	62.5 (5)	31.2 (6)	15.6 (7)	7.8 (8)	Ketoconazole	Negative	Nutrient broth
	***M. oleifera* leaves extract**											
1	*Aspergillus niger*	-	-	-	-	-	+	+	+	-	+	+
2	*Aspergillus flavus*	-	-	-	-	-	+	+	+	-	+	+
3	*Candida albicans*	-	-	-	-	+	+	+	+	-	+	+
4	*Candida glabrata*	-	-	-	+	+	+	+	+	-	+	+
	Bismuth Nanoparticles											
1	*Aspergillus niger*	-	-	-	+	+	+	+	+	-	+	+
2	*Aspergillus flavus*	-	-	-	+	+	+	+	+	-	+	+
3	*Candida albicans*	-	-	-	-	-	+	+	+	-	+	+
4	*Candida glabrata*	-	-	-	-	-	+	+	+	-	+	+

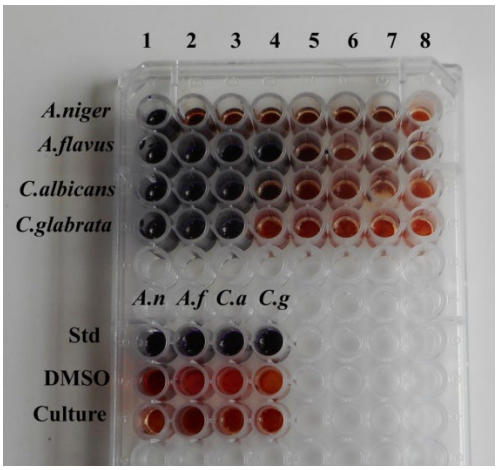

M. oleifera leaves extract

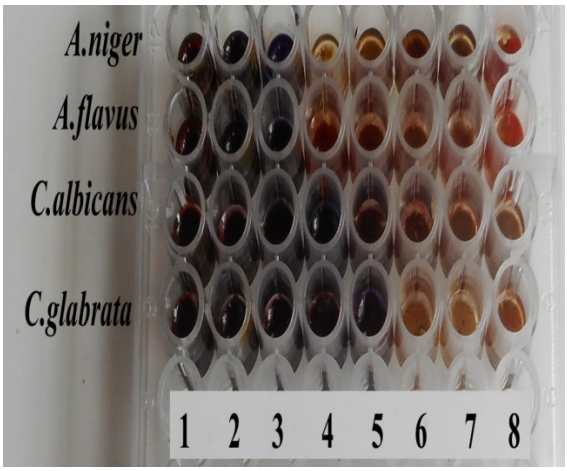

Bismuth nanoparticles

Peer-reviewed version available at *Materials* **2020**, *13*, 876; doi:10.3390/ma13040876

Figure 10. Resazurin microtiter assay plates for the *M. oleifera* leaves extract and the synthesized bismuth nanoparticles.

3. Materials and Methods

3.1. Preparation of the *M. oleifera* Leaves Extract

Fresh *M. oleifera* leaves were collected and shade-dried. The dried leaves were smoothly crushed. The *M. oleifera* leaves powder was stored at room temperature. 10 g of *M. oleifera* leaves powder was taken and soaked in 100 mL water-ethanol (1:1) solution. The mixture was macerated for 1 h and *M. oleifera* leaves extract was filtered through Whatman filter paper 1. The *M. oleifera* leaves extract was used immediately for the preparation of bismuth nanoparticles and other experimental analyses.

3.2. Synthesis of the Bismuth Nanoparticles

Bismuth nitrate pentahydrate (1 g) was dissolved in 20 mL de-mineralized water and added to 80 mL of *M. oleifera* leaves extract. The reaction mixture was stirred for 3 h at 60 °C. The synthesized bismuth nanoparticles were collected by centrifugation and repeatedly washed with de-mineralized water. The synthesized bismuth nanoparticles were dried at 105 °C for 1 h, and subsequently reconstituted in DMSO solvent.

3.3. Characterization of the Size and Morphology of the Synthesized Bismuth Nanoparticles

The completion of synthesis was characterized by UV-Vis spectroscopy. The formation of bismuth nanoparticles and the role of biomolecules in this synthesis were confirmed by BRUKER ALPHA-E FT-IR spectrometry. The crystalline nature of the synthesized bismuth nanoparticles was ascertained using Shimadzu XRD-6000 diffractometer. The size of the

Peer-reviewed version available at *Materials* **2020**, *13*, 876; doi:10.3390/ma13040876

synthesized bismuth nanoparticles was measured by SEM using Quanta 200 FEG scanning electron microscope. The morphology assessment of the synthesized bismuth nanoparticles was done by JEOL JEM-2100 plus transmission electron microscopy. The sample was dispersed in ethanol, coated on the grid, and dried for TEM analysis, along with energy dispersive X-ray analysis.

3.4. Phytochemical Analysis of the *M. oleifera* Leaves Extract

The qualitative analysis of biomolecules present in the *M. oleifera* leaves extract was carried out for the presence of alkaloids, tannins, flavonoids, steroids, saponins, polyphenols, glycosides, carbohydrates, proteins, and amino acids. The total phenolic content in the *M. oleifera* leaves extract was estimated as gallic acid equivalent by Folin-Ciocalteu polyphenol assay [43]. The protein content in the *M. oleifera* leaves extract was estimated by Lowry's method [44].

3.5. Antioxidant Activity

3.5.1. DPPH Assay (Antioxidant Activity Percentage - AA%)

The antioxidant activity percentage (AA%) (scavenging activity) of the *M. oleifera* leaves extract and the synthesized bismuth nanoparticles was assessed by DPPH free radical scavenging assay. 1 mg of ascorbic acid (standard) was dissolved in 1 mL methanol. Different aliquots (serial dilution) of the ascorbic acid solution (0.1-0.5 mL), corresponding to 100-500 µg, were used for calibration. To each tube containing ascorbic acid solution, 1 mL of 0.1 mM DPPH radical solution in ethanol was added, and the final volume was adjusted to 4 mL using ethanol. The stock solutions for the *M. oleifera* leaves extract and the synthesized bismuth nanoparticles were prepared by dissolving 1 mg of each sample in 1 mL of an appropriate solvent (methanol for the *M. oleifera* leaves extract; DMSO for the

synthesized bismuth nanoparticles). Different aliquots from the stock solutions (0.1-0.5 mL), corresponding to 100-500 µg, were added to all tubes except the blank tube (control). The volume in each tube was adjusted to 3 mL using ethanol. To each tube, 1 mL of 0.1 mM DPPH radical solution in ethanol was added. The blank tube (control) was prepared by mixing 3 mL of ethanol and 1 mL of DPPH radical solution in ethanol. All tubes were incubated for 30 min at room temperature, and absorbance at 517 nm was recorded. AA% was determined using the following formula:

AA% = {(absorbance of blank) – (absorbance of sample) / (absorbance of blank)} X 100

3.5.2. Phosphomolybdenum Assay (Total Antioxidant Capacity - TAC)

The total antioxidant capacity (TAC) of the *M. oleifera* leaves extract and the synthesized bismuth nanoparticles was assessed by phosphomolybdenum assay as ascorbic acid equivalent. 1 mg of ascorbic acid (standard) was dissolved in 1 mL methanol. Different aliquots (serial dilution) of the ascorbic acid solution (0.1-0.5 mL), corresponding to 100-500 µg, were prepared. The volume in each tube was adjusted to 4 mL using distilled water.The stock solutions for the *M. oleifera* leaves extract and the synthesized bismuth nanoparticles were prepared by dissolving 1 mg of each sample in 1 mL of an appropriate solvent (methanol for the *M. oleifera* leaves extract; DMSO for the synthesized bismuth nanoparticles). Different aliquots from the stock solutions (0.1-0.5 mL), corresponding to 100-500 µg, were added to all tubes except the blank tube (control). The volume in each tube was adjusted to 3 mL using distilled water. To each tube, 1 mL of phosphomolybdenum reagent (0.6 M sulphuric acid, 28 mM sodium phosphate, and 4 mM ammonium molybdate) was added. The volume in each tube was adjusted to 4 mL using distilled water. After incubation for 90 min at 95°C, absorbance at 695 nm was recorded. The calibration curve for the ascorbic acid solution (standard) was plotted for the absorbance at 695 nm against known

Peer-reviewed version available at *Materials* **2020**, *13*, 876; doi:10.3390/ma13040876

amounts of ascorbic acid with the phosphomolybdate reagent, so as to express the TAC values as ppm equivalent of ascorbic acid. Using the ascorbic acid calibration curve, the TAC values for the *M. oleifera* leaves extract and the synthesized bismuth nanoparticles were calculated and expressed as ppm equivalent of ascorbic acid.

3.6. Anti-Bacterial Activity using Resazurin Microtiter Assay

The bacterial cultures of *Escherichia coli*, *Klebsiella pneumoniae*, *Staphylococcus aureus*, and *Enterococcus faecalis* were obtained from the Royal Bio Research Centre, Chennai, Tamil Nadu, India. The most rapid and inexpensive way to screen several microorganism isolates at the same time, with better correlation in comparison to other techniques, is the resazurin microtiter assay [45-47]. The resazurin solution was prepared by dissolving a 270 mg tablet of resazurin in 40 mL of sterile distilled water. The test was carried out in 96-well plates under aseptic conditions. A volume of 100 µL of sample containing 10 mg/mL was pipetted into the first well of the plate. To all other wells, 50 µL of nutrient broth was added, and the tested sample was serially diluted. Subsequently, 10 µL of resazurin solution and 10 µL of bacterial suspension were added to each well. Each plate was wrapped loosely with cling film to prevent dehydration. The plates were incubated at 37°C for 18-24 h. The color change was then assessed visually. A color change from purple to pink (or colorless) was recorded as positive, indicating cell growth (i.e. (+) means growth and (-) means no growth). MIC was set to be the lowest concentration at which color change occurred. Streptomycin (10 µg/500 µL) was used as a positive control, while water-ethanol (1:1) solution and DMSO solvent were used as negative controls for the *M. oleifera* leaves extract and the bismuth nanoparticles, respectively. The nutrient broth was also used as a negative control.

3.7. Anti-Fungal Activity using Resazurin Microtiter Assay

Peer-reviewed version available at *Materials* **2020**, *13*, 876; doi:10.3390/ma13040876

The fungal cultures of *Aspergillus niger*, *Aspergillus flavus*, *Candida albicans*, and *Candida glabrata* were obtained from the Royal Bio Research Centre, Chennai, Tamil Nadu, India. The resazurin microtiter assay was performed as described above (section 3.6). Ketoconazole (10 µg/500 µL) was used as a positive control, while water-ethanol (1:1) solution and DMSO solvent were used as negative controls for the *M. oleifera* leaves extract and the bismuth nanoparticles, respectively.The nutrient broth was also used as a negative control.

4. Conclusion

Our experimental approach led to the successful green synthesis of bismuth nanoparticles using a hydroalcoholic extract of *M. oleifera* leaves.UV-Vis absorption and FT-IR spectrometry confirmed the formation of bismuth nanoparticles and the role of different biomolecules present in the *M. oleifera* leaves extract in the synthesis of bismuth nanoparticles. The presence of elemental bismuth was affirmed by the energy dispersive X-ray spectroscopy analysis (EDS).XRD confirmed the crystalline nature of the synthesized bismuth nanoparticles. SEM analysis revealed that the size of the synthesized bismuth nanoparticles is in the range of 40.4-57.8 nm. As revealed by TEM with EDS, the synthesized bismuth nanoparticles were confirmed to display an amorphous morphology. DPPH and phosphomolybdenum assays revealed that both the *M. oleifera* leaves extract and the synthesized bismuth nanoparticles exert antioxidant activity. However, the antioxidant activity of the synthesized bismuth nanoparticles is weaker than that of the *M. oleifera* leaves extract, probably due to a loss of some phenolic constituents. Our study also revealed that the *M. oleifera* leaves extract and the synthesized bismuth nanoparticles play potent anti-bacterial role against *E. coli*, *K. pneumoniae*, *S. aureus* and *E. faecalis* (MIC values for the extract: 500, 250, 250, and 250 µg/mL; MIC values for the bismuth nanoparticles: 500, 500, 500, and 250 µg/mL, respectively), with a more profound inhibitory effect of the bismuth nanoparticles,

Peer-reviewed version available at *Materials* **2020**, *13*, 876; doi:10.3390/ma13040876

compared to the *M. oleifera* leavesextract, against *E. faecalis*. Moreover, our findings also revealed that the *M. oleifera* leaves extract and the synthesized bismuth nanoparticles display relatively stronger anti-fungal activity against *A. niger*, *A. flavus*, *C. albicans* and *C. glabrata* (MIC values for the extract: 62.5, 62.5, 125, and 250 µg/mL; MIC values for the bismuth nanoparticles: 250, 250, 62.5, and 62.5 µg/mL, respectively), with a promising and exploitable inhibitory activity against Candida species. This indicates that the anti-fungal activity of the *M. oleifera* leaves extract against *A. niger* and *A. flavus* is stronger than that of the synthesized bismuth nanoparticles, while the latter exert more potent anti-fungal activity against *C. albicans* and *C. glabrata*. Obviously, the green synthesis of bismuth nanoparticles using a hydroalcoholic extract of *M. oleifera* leaves did not jeopardize the bismuth nanoparticles' anti-bacterial and anti-fungal activities. Collectively, our study suggests that the synthesized bismuth nanoparticles can potentially be employed in the amelioration of oxidative stress and various microbial infections. In particular, the synthesized bismuth nanoparticles seem to be powerful anti-fungal agents against cases of candidiasis including, but not limited to, oral thrush, urinary yeast infection, genital infection, intra-abdominal candidiasis, acute hematogenous candidiasis, fungemia, invasive candidiasis, endocarditis, and endophthalmitis.

Acknowledgments

We acknowledge the HRTEM Facility at SRMIST set up with support from MNRE (Project No. 31/03/2014-15/PVSE-R&D), Government of India. We acknowledge Nanotechnology Research Centre (NRC), SRMIST for providing the research facilities.

Author Contributions

Peer-reviewed version available at *Materials* **2020**, *13*, 876; doi:10.3390/ma13040876

N.S., I.A.A.Y, A.F.M., and P.P. designed the experiments and supervised their execution. P.E.D. performed the preparation of the *M. oleifera* leaves extract and the green synthesis of the copper nanoparticles. P.E.D. performed the phytochemical and biological analyses. P.E.D., N.S., I.A.A.Y, A.F.M., and P.P. performed data analyses of the experimental assays. All authors contributed to manuscript writing and preparation.

Conflicts of Interest

The authors declare no conflicts of interest.

References

1. Rathi, B.S.; Bodhankar, S.L.; Baheti, A.M. Evaluation of aqueous leaves extract of *Moringa oleifera* Linn for wound healing in albino rats. *Indian J. Exp. Biol.* **2006**, *44*, 898-901.
2. Ogbe, A.O.; Affiku, J.P. Proximate study, mineral and anti-nutrient composition of *Moringa oleifera* leaves harvested from Lafia, Nigeria: potential benefits in poultry nutrition and health. *JMBFS* **2011**, *1*(3), 296-308.
3. Siddhuraju, P.; Becker, K. Antioxidant properties of various solvent extracts of total phenolic constituents from three different agroclimatic origins of drumstick tree (*Moringa oleifera* Lam.) leaves. *J. Agric. Food Chem.* **2003**, *51*, 2144-2155.
4. Fitzgerald, D.J.; Stratford, M.; Gasson, M.J.; Ueckert, J.; Bos, A.; Narbad, A. Mode of antimicrobial action of vanillin against *Escherichia coli*, *Lactobacillus plantarum* and *Listeria innocua*. *J. App. Microbiol.* **2004**, *97*, 104–113.
5. Narasimhan, S.; Maheshwaran, S.; Abu-Yousef, I.A.; Majdalawieh, A.F.; Rethavathi, J.; Das, P.E.; Poltronieri, P. Anti-bacterial and anti-fungal activity of xanthones obtained via

semi-synthetic modification of α-mangostin from *Garcinia mangostana*. *Molecules* **2017**, *22*(2), E275.

6. Suwantong, O.; Pankongadisak, P.; Deachathai, S.; Supaphol, P. Electrospun poly(l-lactic acid) fiber mats containing crude *Garcinia mangostana* extracts for use as wound dressings. *Polym. Bull.* **2014**, *71*, 925-949.
7. Lakouraj, M.M.; Rahpaima, G.; Mohseni, M. Synthesis, characterization, metal sorption, and biological activities of organosoluble and thermally stable azoxanthone-based polyester. *Polym. Adv. Tech.* **2015**, *26*, 3, 234-244.
8. Mun, S.H.; Joung, D.K.; Kim, Y.S.; Kang, O.H.; Kim, S.B.; Seo, Y.S.; Kwon, D.Y. Synergistic antibacterial effect of curcumin against methicillin-resistant *Staphylococcus aureus*. *Phytomedicine* **2013**, *20*, 714-718.
9. Dogra, N.; Choudhary, R.; Kohli, P.; Haddock, J.D.; Makwana, S.; Horev, B.; Vinokur, Y.; Droby, S.; Rodov, V. Polydiacetylene nanovesicles as carriers of natural phenylpropanoids for creating antimicrobial food-contact surfaces. *J. Agr. Food Chem.* **2015**, *63*, 2557-2565.
10. Ravichandran, M.; Hettiarachchy, N.S.; Ganesh, V.; Ricke, S.C.; Singh, S. Enhancement of antimicrobial activities of naturally occurring phenolic compounds by nanoscale delivery against *Listeria monocytogenes*, *Escherichia coli* O157:H7 and *Salmonella Typhimurium* in broth and chicken meat system. *J. Food Safety* **2011**, *31*, 462-471.
11. Horev, B.; Sela, S.; Vinokur, Y.; Gorbatsevich, E.; Pinto, R.; Rodov, V. The effects of active and passive modified atmosphere packaging on the survival of *Salmonella enterica* serotype Typhimurium on washed romaine lettuce leaves. *Food Res. Int.* **2012**, *45*, 1129-1132.
12. Fadida, T.; Kroupitski, Y.; Peiper, U.M.; Bendikov, T.; Sela, S.; Poverenov, E. Air-ozonolysis to generate contact active antimicrobial surfaces: activation of polyethylene

and polystyrene followed by covalent graft of quaternary ammonium salts. *Colloids Surf. B Biointerfaces* **2014**, *122*, 294-300.

13. Meridor, D.; Gedanken, A. Preparation of enzyme nanoparticles and studying the catalytic activity of the immobilized nanoparticles on polyethylene films. *Ultrason. Sonochem*. **2013**, *20*, 425-431.
14. Reidy, B.; Haase, A.; Luch, A.; Dawson, K.A.; Lynch, I. Mechanisms of silver nanoparticle release, transformation and toxicity: a critical review of current knowledge and recommendations for future studies and applications. *Materials* **2013**, *6*, 2295-2350.
15. Malka, E.; Perelshtein, I.; Lipovsky, A.; Shalom, Y.; Naparstek, L.; Perkas, N.; Patick, T.; Lubart, R.; Nitzan, Y.; Banin, E.; Gedanken, A. Eradication of multi-drug resistant bacteria by a novel Zn-doped CuO nanocomposite. *Small* **2013**, *9*, 4069-4076.
16. Borase, H.P.; Salunke, B.K.; Salunkhe, R.B.; Patil, C.D.; Hallsworth, J.E.; Kim, B.S.; Patil, S.V. Plant extract: a promising bio-matrix for ecofriendly, controlled synthesis of silver nanoparticles. *Appl. Biochem. Biotechnol.* **2014**, *17*, 1-29.
17. Park, Y. A new paradigm shift for the green synthesis of antibacterial silver nanoparticles utilizing plant extracts. *J. Korean Soc. Toxicol. Res.* **2014**, *30*(3), 169-178.
18. Mohanta, Y.K.; Panda, S.K.; Jayabalan, R.; Sharma, N.; Bastia, A.K.; Mohanta, T.K. Antimicrobial, antioxidant and cytotoxic activity of silver nanoparticles synthesized by leaf extract of *Erythrina suberosa* (Roxb.). *Front. Mol. Biosci.* **2017**, *4*, 1-9.
19. Madhavaraj, L.; Sethumadhavan, V.V.; Geun, H.G.; Mathur, N.K.; Si, W.K. Synthesis, characterization and evaluation of antimicrobial efficacy of silver nanoparticles using *Paederia foetida* leaf extract. *Intern. Res. J. Biol. Sci* .**2013**, *15*(3), 76-80.
20. Krishnaraj, C.; Jagan, E.G.; Rajasekar, S.; Selvakumar, P.; Kalaichelvan, P.T.; Mohan, N. Synthesis of silver nanoparticles using *Acalypha indica* leaf extracts and its antibacterial activity against water borne pathogens. *Colloids Surf. B: Biointerfaces* **2010**, *76*, 50-56.

21. Parveen, A.; Roy, A.S.; Rao, S. Biosynthesis and characterization of silver nanoparticles from *Cassia auriculata* leaf extract and *in vitro* evaluation of antimicrobial activity. *Intern. J. Appl. Biol. Pharmaceutical Technol.* **2012**, *3*(2), 222-228.

22. Dubey, S.P.; Lahtinen, M.; Särkkä, H.; Sillanpää, M. Bioprospective of *Sorbus aucuparia* leaf extract in development of silver and gold nanocolloids. *Colloids Surf. B: Biointerfaces* **2010**, *80*(1), 26-33.

23. Gavhane, A.J.; Padmanabhan, P.; Kamble, S.P.; Jangle, S.N. Synthesis of silver nanoparticles using the extracts of neem leaf and triphala and the evaluation of their antimicrobial activities. *Int. J. Pharm. Biol. Sci.* **2012**, *3*, 88-100.

24. Ahmed, S.; Ahmad, M.; Swami, B.L.; Ikram, S. A review on plants extract mediated synthesis of silver nanoparticles for antimicrobial applications: a green expertise. *J. Adv. Res*., **2016**, *7*, 17-28.

25. Mohanta, Y.K.; Panda, S.K.; Biswas, K.; Tamang, A.; Bandyopadhyay, J.; De, D. Biogenic synthesis of silver nanoparticles from *Cassia fistula* (Linn.): *in vitro* assessment of their antioxidant, antimicrobial and cytotoxic activities. *IET Nanobiotechnol*. **2016**, *10*(6), 438-444.

26. Mariselvam, R.; Ranjitsingh, A.J.; Usha Raja Nanthini, A.; Kalirajan, K.; Padmalatha, C.; Mosae Selvakumar, P. Green synthesis of silver nanoparticles from the extract of the inflorescence of *Cocos nucifera* (Family: Arecaceae) for enhanced antibacterial activity. *Spectrochim. Acta A Mol. Biomol. Spectrosc.* **2014**, *129*, 537-541.

27. Balashanmugam, P.; Caral Dinesh, R.; Manivasagan, V.; Ramesh Babu, N.G.; Kalaichelvan, P.T. Extracellular biosynthesis of silver nanoparticles using *Cassia fistula* extract and *in vitro* antimicrobial studies. *J. Pharm. Res*. **2014**, *8*(2), 187-191.

Peer-reviewed version available at *Materials* **2020**, *13*, 876; doi:10.3390/ma13040876

28. Majeed, A.; Ullah, W.; Anwar, A.W.; Shuaib, A.; Ilyas, U.; Khalid, P. Cost-effective biosynthesis of silver nanoparticles using different organs of plants and their antimicrobial applications: a review. *Mater. Technol.* **2016**, *33*, 313-320.
29. Torrisi, L.; Silipigni, L.; Restuccia, N.; Cuzzocrea, S.; Cutroneo, M.; Barreca, F.; Fazio, B.; Di Marco, G.; Guglielmino, S. Laser-generated bismuth nanoparticles for applications in imaging and radiotherapy. *J. Phys. Chem. Solids* **2018**, *119*, 62-70.
30. Zhao, Y.; Zhang, Z.; Dang, H. A simple way to prepare bismuth nanoparticles. *Mater. Lett.* **2004**, *58*, 790-793.
31. Pothula, K.; Tang, L.; Zha, Z.; Wang, Z. Bismuth nanoparticles: an efficient catalyst for reductive coupling of nitroarenes to azo-compounds. *RSC Adv.* **2015**, *5*, 83144-83148.
32. Rieznichenko, L.S.; Gruzina, T.G.; Dypkova, S.M., Ushkalov, V.O.; Ulberg, Z.R. Investigation of bismuth nanoparticles antimicrobial activity against high pathogen microorganism. *American J. Bioterror. Biosecur. Biodefens.* **2015**, *2*(1), 1004.
33. Xia, F.; Xu, X.; Li, X.; Zhang, L.; Zhang, L.; Qiu, H.; Wang, W.; Liu, Y.; Gao, J. Preparation of bismuth nanoparticles in aqueous solution and its catalytic performance for the reduction of 4-nitrophenol. *Ind. Eng. Chem. Res*. **2014**, *53*(26), 10576-10582.
34. Liang, Y.; Manioudakis, J.; Macairan, J.R.; Askari, M.S.;Forgione, P.; Naccache, R. Facile aqueous-phase synthesis of an ultrasmall bismuth nanocatalyst for the reduction of 4-nitrophenol. *ACS Omega* **2019**, *4*(12), 14955-14961.
35. Ruiz-Ruiz, V-F.; Zumeta-Dubé, I.; Díaz, D.; Arellano-Jiménez, M.J.; José-Yacamán. M. Can silver be alloyed with bismuth on nanoscale? An optical and structural approach. *J. Phys. Chem. C* **2017**, *121*(1), 940-949.
36. Manasa, M.G.; Bhakta, A.K.; Mekhalif, Z.; Mascarenhas, R.J. Bismuth-nanoparticles decorated multi-wall-carbon-nanotubes cast-coated on carbon paste electrode; an

electrochemical sensor for sensitive determination of gallic Acid at neutral pH. *Mater. Sci. Energy Technol.* **2020**, *3*, 174-182.

37. Reverberi, A.P.; Varbanov, P.S.; Lauciello, S.; Salerno, M.; Fabiano, B. An eco-friendly process for zerovalent bismuth nanoparticles synthesis. *J. Clean. Prod.* **2018**, *198*, 37-45.
38. Torrisi, L.; Silipigni, L.; Restuccia, N.; Cuzzocrea, S.; Cutroneo, M.; Barreca, F.; Fazio, B.; Di Marco, G.; Guglielmino, S. Laser-generated bismuth nanoparticles for applications in imaging and radiotherapy. *J.Phys. Chem. Solids* **2018**, *119*, 62-70.
39. Gomez, C.; Hallot, G.; Port, M. Inorganic frameworks as smart nanomedicines, Chapter 10 Bismuth metallic nanoparticles. Edited by Alexandru Mihai Grumezescu, William Andrew. Applied Science Publishers, London, UK. **2018**, pp. 449-487.
40. Moyo, B.; Masika, P.J.; Hugo, A.; Muchenje, V. Nutritional characterization of Moringa (Moringa *oleifera* Lam.) leaves. *Afr. J. Biotechnol*. **2011**, *10*(60), 12925-12933.
41. Rodríguez-Pérez, C.;Quirantes-Piné, R.; Fernández-Gutiérrez, A., Segura-Carretero, A. Optimization of extraction method to obtain a phenolic compounds-rich extract from *Moringa oleifera* Lam leaves. *Ind. Crop. Prod.* **2015**, *66*, 246-254.
42. Vongsak, B.; Sithisarn, P.; Gritsanapan, W. Simultaneous HPLC quantitative analysis of active compounds in leaves of *Moringa oleifera* Lam. *J. Chromatogr. Sci.* **2013**, *52*(7), 641-645.
43. Koşar, M.; Dorman, H.J.D.; Hiltunen, R. Effect of an acid treatment on the phytochemical and antioxidant characteristics of extracts from selected Lamiaceae species. *Food Chem.* **2005**, *91*, 525-533.
44. Lowry, O.H.; Roserbough, N.J.; Farr, A.L.; Randall, R.J. Protein measurement with the folin phenol reagent. *J. Biol. Chem.* **1951**, *193*, 265-275.
45. Monteiro, M.C.; de la Cruz, M.; Cantizani, J.; Moreno, C.; Tormo, J.R.; Mellado, E.; De Lucas, J.R.; Asensio, F.; Valiante, V.; Brakhage, A.A.; Latgé, J.P.; Genilloud, O.; Vicente

F. A new approach to drug discovery: high-throughput screening of microbial natural extracts against *Aspergillus fumigatus* using resazurin. *J. Biomol. Screen.* **2012**, *17*(4), 542-549.

46. Sarker, S.D.; Nahar, L.; Kumarasamy, Y. Microtitre plate-based antibacterial assay incorporating resazurin as an indicator of cell growth, and its application in the *in vitro* antibacterial screening of phytochemicals. *Methods* **2007**, *42*(4), 321-324.
47. Hudman, D.A.; Sargentini, N.J. Resazurin-based assay for screening bacteria for radiation sensitivity. *Springerplus* **2013**, 2(1), 55.